Response letter (manuscript #APL24-AR-06899)

We would like to thank the reviewers for their valuable feedback and insightful comments. Their suggestions have greatly contributed to improving the quality of our manuscript. Our response to each comment is explained below, and the revisions are marked in red in the submitted manuscript.

Reviewer #1

Optional Suggestions for Improvement

Comment 1) Clarification of Field Direction in Figure 2c: In Figure 2c, the direction of the applied magnetic field (H) is not clearly indicated. I assume it is along the x-direction, but a clarification in the figure caption would enhance the reader's understanding.

(Response) We have added "H was applied in the x direction" in the caption of Fig. 2(c). Also, the label the x-axis of Fig. 2(c) has been replaced with $\mu_0 H_x$ from $\mu_0 H$ (added subscript x).

Comment 2) Impact of Stray Fields on Sensitivity: For practical sensor applications, it would be beneficial to discuss how the sensitivity of the TMR transfer curve changes in response to disturbing stray fields, particularly in the orthogonal (y) direction. This would provide a more comprehensive understanding of the sensor's performance in real-world environments.

(Response) Thank you very much for the insightful suggestion. We have simulated the R-H_x curve under a constant magnetic field in the y direction (H_y).

Assumption: $J_f = 0.1$ mJ/m^2, $J_1 = J_2 = -0.35$ mJ/m^2 (then, $\theta_{ud} = 120°$ from Eq. (S8)), $K_u t_{FL} = 0.03$ mJ/m^2, and $\theta_{ua} = 60°$.

(1) When $H_x = 0$, $\mathbf{m}_{FL}$ is stabilized in the state of the blue arrow ($\theta_{FL} = 90°$), as shown in Fig. R1(a), by the balance of the unidirectional and uniaxial anisotropies.

(2) We simulate R-H_x curves under constant H_y (-10 mT $\leq \mu_0 H_y \leq 10$ mT)

Figure R1(b) shows the R-H_x curves under positive H_y. The sensitivity dR/dH_x decreased with increasing H_y. This was because the positive H_y acted as an additional anisotropy field for $\mathbf{m}_{FL}$.

Figure R1(c) shows the R-H_x curves under negative H_y. For $\mu_0 H_y = -1.0$ mT, the sensor got higher sensitivity, which is understood by the reduced anisotropy field due to the negative H_y. For $\mu_0 H_y$ between -1.5 mT and -7.0 mT, the R-H_x curves exhibited hysteresis. The hysteretic R-H_x curves can be understood by the dependence of θ_{FL} on the strength and sweep direction of H_x, as shown in Fig. R1(d) for $\mu_0 H_y = -1.5$ mT. When $\mu_0 H_x$ was swept from +10 mT to -10 mT (black curve), θ_{FL} increasedd from ~0 to 180°. On the other hand, when $\mu_0 H_x$ was swept from

–10 mT to +10 mT (red curve), θ_{FL} increased from 180 to ~360°. Therefore, $\mathbf{m}_{FL}$ followed different paths, creating hysteresis in the R-H_x curve.

This is important from an application point of view. However, discussing this is beyond the scope of this letter, and the space is limited. We would like to discuss this with experimental data in our future publication.

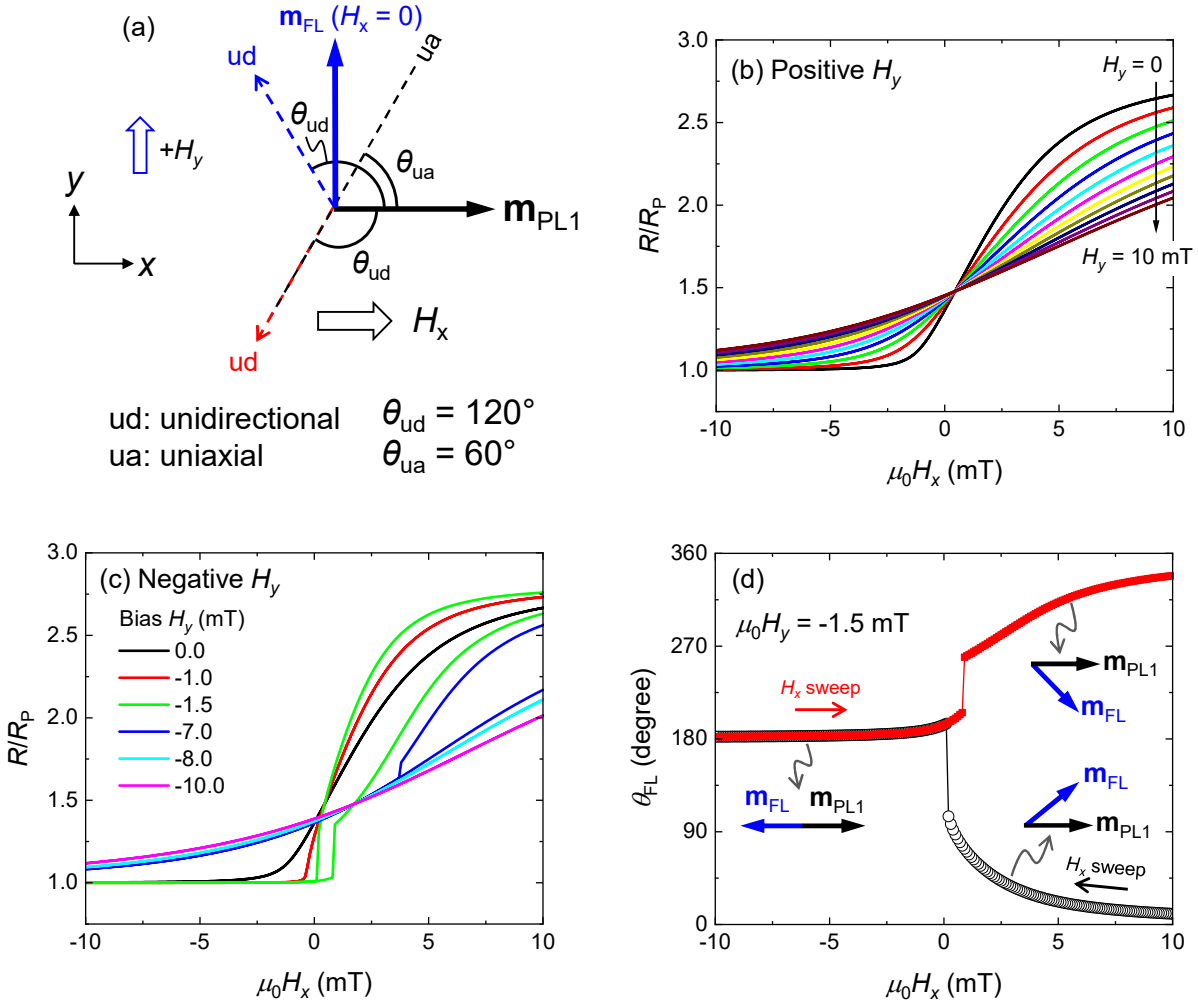

FIG. R1. (a) Magnetization and anisotropy direction diagram. Simulated R-H_x curves under a (b) positive and (c) negative H_y. R is normalized by the value in the parallel magnetization state (R_P). (d) Dependences of θ_{FL} on the strength and sweep direction of H_x for $\mu_0 H_y$ = –1.5 mT.

Comment 3) Clarification in Figure 3e and 3f: The contour plot in Figure 3 suggests that the device in panel (e) exhibits higher sensitivity than the device in panel (f), as indicated by the green versus blue color. However, the experimental data in Figures 3e and 3f seem to suggest the opposite. This discrepancy could be due to differences in the RuFe composition between the two devices. I recommend clarifying whether both the annealing directions and the RuFe compositions were altered between these two experiments to ensure the results are interpreted correctly.

(Response) The contour plot in Fig. 3(c) shows the sensitivity at H =0. The devices in Figs. 3(e) and (f) show sensitivities at H = 0 of 21 %/mT and 14 %/mT, respectively. The trend of these values is qualitatively consistent with the simulated values ((e) 28 %/mT and 7 %/mT). The quantitative difference in the sensitivity value between the experiment and simulation may be due to the values of the anisotropy energies used for the simulation. These results demonstrate that the R-H simulation is a useful tool for designing the noncollinear IEC angle (θ_{ua}) and uniaxial anisotropy angle (θ_{ua}).

The different annealing angle for these devices has been explain in the original manuscript: (p.10, line 6-9)

"The angles of the magnetic anisotropies were θ_{ud} ~130° and θ_{ua} = 40° for the $Ru_{40}Fe_{60}$ spacer, and θ_{ud} ~120° and θ_{ua} = 120° for the $Ru_{35}Fe_{65}$ spacer. θ_{ud} were estimated by fitting the M–H curves (not shown here), and θ_{ua} was controlled by the annealing process."

For clarification, we have added the values of sensitivity at H = 0 as follows: (p.10, line 12-15)

"For the $Ru_{40}Fe_{60}$ spacer, the highest sensitivity state (21 %/mT) was obtained at around H = 0, … On the other hand, the device with the $Ru_{35}Fe_{65}$ spacer showed a relatively low sensitivity at H = 0 (14 %/mT)

Reviewer #2

Major comments

My main concern relates to the significance of your manuscript contribution.

Comment 1) You wrote that the method (here I call it 2AFM-2ANN) for achieving orthogonal configuration between magnetizations of free and reference layers based on induction of unidirectional anisotropy requires two antiferromagnets (AFM) and a two step annealing process.

However, your proposed TMR devices with noncollinear interlayer exchange coupling structure, which allows for orthogonal magnetization configurations and low hysteresis, also used two AFMs and required two annealing steps.

Thus, what is the advantage of your design based on the noncollinear interlayer exchange coupling as compared to the 2AFM-2ANN?

(Response) Thank you for pointing out the ambiguity of our argument. The significance of this paper is (1) providing a new linearization method of the *R-H* curve of TMR sensor devices using exchange bias and noncollinear IEC, and (2) revealing the effect of the direction of uniaxial anisotropy to control the TMR curve shape and reduce hysteresis.

Thanks to your comment, we realized that our manuscript contained misleading descriptions and lacked clear statements about the proposed sensor design and 2AFM-ANN design. Therefore, we have made the following revisions.

First, the description in the original manuscript: "However, this method (2AFM-2ANN) requires two AFM layers with different blocking temperatures and a double annealing process, …" gives the wrong impression that the proposed method in this paper does not use two AFM layers and two-step annealing. Therefore, we have deleted the above sentence and revised it as follows: (p.3, line 5-10)

"Another sensor design where the FL is stabilized by unidirectional anisotropy (exchange bias) results in a single-domain state of FL magnetization, causing a considerably smaller magnetic hysteresis.[12,13,20,21] These sensors achieve an orthogonal magnetization configuration between the FL and reference layer (RL) using two AFM layers with different blocking temperatures processed by two-step annealing."

Second, we think that the difference between 2AFM-2ANN sensors and the proposed sensor in various aspects are as follows:

[Requirement of two AFM layers]

The "2AFM-2ANN" design requires two AFM layers with different blocking temperatures (T_b), which is typically achieved by two different AFM materials, (*) such as PtMn and IrMn, as reported by [Wang, JAP 99, 08H703 (2006)] and [Ferreira, IEEE Trans. Magn. 48, 3719 (2012)]. The need for two expensive AFM materials increases the cost for manufacturing the sensors.

One the other hand, the proposed sensor also requires two AFM layers but does not require different T_b. Therefore, a single AFM material, such as IrMn, is sufficient. This can be a cost advantage for the manufacturing.

*Note that [Chen, APL 100, 142407 (2012)]obtained a 2AFM-2ANN sensor using two IrMn layers with different T_b, which was achieved by differences in the IrMn thickness and microstructure. However, a well-separated T_b by different AFM materials is considered to be preferable in terms of the robustness in sensor fabrication and the stability of sensor properties. In fact, the second annealing temperature in the Chen's paper was 150 °C, indicating T_b < 150 °C for one of the IrMn layers. Such a low T_b may be of concern in terms of the reliability of the pinning stability in harsh environments.

[Two-step annealing]

In a simple picture, as we initially expected, the proposed design with noncollinear IEC needs only a single annealing process (one temperature and one magnetic field direction), but it actually needs two annealing steps due to the importance of controlling the uniaxial anisotropy.

The two-step annealing for 2AFM-2ANN sensors can be done by a single loading to annealing oven with a function of the rotation of magnetic field. Therefore, the proposed sensor design has no practical advantage in terms of the process duration for annealing. We apologize for the misleading statements in the previous manuscript. We have removed the statements of "single annealing process" in the entire manuscript.

[Hysteresis]

Both our devices and the reported 2AFM-2ANN devices show small coercivity (H_c) for the full loops due to the unidirectional anisotropy of the FLs. Our devices showed **H_c = 0.02 mT (Fig. 3(e)** and **~0 (Fig. 3(f) and Fig. S2) for the device of Fig. 4(b))**. These values are smaller than those of the reported 2AFM-2ANN with two-step annealing: H_c ~ 0.1 mT [Ferrira 2012, Silva EPJ Appl. Phys. **72**, 10601 (2015)] and ~1 mT [Chen 2009]. However, since H_c depends on the FL materials as well as the magnetization stabilization mechanism, appealing the smaller H_c of our devices compared to those of the reported 2AFM-2ANN devices lacks the scientific validity. Therefore, we believe that we should not compare the H_c values of the present devices and 2AFM-2ANN devices in this paper.

[Control of FL anisotropy field]

2AFM-2ANN sensors use an ultrathin Ru ducting layer to control the FL pinning (anisotropy) field. As reported previously, the FL pinning field changes significantly with every half Å of the Ru dusting layer, which could be a challenge for stability in mass production.

On the other hand, in the sensors proposed in this paper, the FL anisotropy is controlled by the orange-peel ferromagnetic coupling thorough the AgSn spacer. The ferromagnetic coupling strength of FL shows a relatively mild dependence on the AgSn spacer thickness. [Nakatani, APL 121, 192406 (2022)] Thus, the control of the FL anisotropy field to small values for high sensitivity may be more stable for the proposed sensor. In the present study, we did not attempt to vary the sensitivity by the AgSn spacer thickness, which is our future plan of study.

[Reliability]

We have pointed out in the manuscript that the proposed sensor has a problem that the *R*-*H* curves change by apply a set field in *y* direction, as discussed based on Fig. 4. There is no such concern for the 2AFM-2ANN sensors. We are not aware of any reliability concerns for the 2AFM-2ANN sensors based on the publications (we have no experience with 2AFM-2ANN sensors).

As discussed above, we can point out some potential advantages of the proposed sensor design with noncollinear IEC over the 2AFM-2ANN design. However, it is not appropriate to discuss these technical perspectives in this paper without showing concrete data through a fair comparison. Therefore, in the revised manuscript, we describe the general facts as follows:

(p12, line14-)

"The present devices achieve essentially the same function as the sensors with soft-pinned FLs,[12,13,20,21] in terms of linear *R*–*H* curves with negligible hysteresis. The soft-pinned FL sensors obtain unidirectional FL anisotropy orthogonal to the RL magnetization by two-step annealing for two AFM layers with different blocking temperatures, e.g., PtMn and IrMn layers.

The strength of the FL anisotropy field is controlled by the thickness of the ultrathin dusting layer, typically with Ru, inserted between the AFM layer and the FL. On the other hand, the present devices achieve a noncollinear magnetization configuration between the FL and RL by exchange bias transferred via a noncollinear IEC through the RuFe spacer. The FL anisotropy field is controlled by the strength of the orange-peel FM coupling through the thickness of the AgSn non-magnetic spacer. These two types of sensor designs may have different advantages and challenges depending on the required sensor characteristics such as sensitivity and dynamic range. Therefore, for specific applications, various technical and economic aspects such as sensing characteristics, reliability, manufacturability, and cost must be evaluated."

Comment 2) You claim that the TMR device with noncollinear interlayer exchange coupling structure reduces the hysteresis. You showed the device's TMR-H curve, but you did not quantify the hysteresis and compare it to the hysteresis of the devices based on 2AFM-2ANN.

(Response) We have added the coercivity (H_c) values of the TMR devices as described below. Our argument in this paper is that tilting the direction of uniaxial anisotropy away from the pinning direction reduces the H_c of the TMR curve. We do not intend to compare the H_c values of our devices with those of the 2AFM-2ANN sensors. As mentioned above **[Hysteresis]**, the H_c values of the present devices are lower than those of the 2AFM-2ANN sensors in the literature. However, since H_c is greatly influced by the FL material, it is not valid to compare these H_c values with different FL materials.

(p.10, line 9-13)
"Compared to the device with $\theta_{ua} = 0$, which exhibited $\mu_0 H_c = 0.23$ mT [Fig. 2(c)], these device with $\theta_{ua} \neq 0$ showed significantly reduced hysteresis: $\mu_0 H_c \sim 0.02$ mT for the $Ru_{40}Fe_{60}$ spacer and $\mu_0 H_c \sim 0$ mT for the $Ru_{35}Fe_{65}$ spacer, as shown in the insets of Figs. 3(e) and (f), respectively."

Comment 3) The structure of the TMR devices you propose consists of 17 active layers of 12 different materials, which is very complex for potential sensor applications.

(Response) The multilayer structure of the present devices is the result of our stack developments to improve the function of each component, such as pinning (CoFe inserted below Co in PL1), softmagnetism of FL (amorphous CoFeBTa), TMR ratio (Ta (0.3 nm) inserted in PL and RL). These films were deposited from eight sputtering targets: Ta, Ru, IrMn, Co, Fe, CoFeB, MgO, and AgSn. The RuFe, CoFe, and CoFeBTa layers were co-sputtered. Such a number of sputtering targets and co-sputtering process are available in TMR manufacturing sputtering tools, such as Cannon Anelva C7100.

However, the proposed sensor design requires 11 layer-elements of AFM1/PL1/RuFe/PL2/AgSn/FL/MgO/RL/Ru/PL3/AFM1, excluding the seed and capping layers. This is more than that of the 2AFM-2ANN design: AFM1/Ru-dust/FL/MgO/RL/Ru/PL/AFM2 (8 elements). Although the complication of the layer structure

does not affect the scientific value of this study, we have added the following comment in the revised manuscript.

(p. 13, line 1-2)
"Therefore, for specific applications, various technical and economic aspects such as sensing characteristics, reliability, manufacturability, and cost must be evaluated."

Comment 4) Moreover, the manuscript lacks citations to works that proposed to use interference perpendicular anisotropy to achieve orthogonal magnetizations configuration just by thinning the free layer.

(Response) Thanks for pointing out our mistake. We have added the following papers in the introduction part of this manuscript.

(p.2, line) "… perpendicular magnetic anisotropy,[16,17]…"
[16] Wisniowski et al., IEEE Trans. Magn. 48, 3840 (2012)
[17] Wisniowski et al., J. Appl. Phys. 122, 213906 (2017)

Minor comments

1. To improve reading and clarity, please rewrite the manuscript text into single topic paragraphs with clearly stated topic sentences and concise sentences. Please split some non-single topics.

(Response) We have split long paragraphs as follows. Also, the manuscript has been edited by a professional proofreading service, Editage.
(p. 2-3) "Magnetization stabilization…" and "Uniaxial…"
(p. 8-9) "Note that annealing…" and "Figure 3(e) shows…"

2. In Fig. 3 e), f) show plot of experimental TMR-H curves in zoomed range of field (0-4 Oe).

(Response) We have added the zoomed-in TMR curves with field range ±0.2 mT in the insets of Figs. 3(e) and (f). For the device shown in Fig. 4, we added the full loop in Fig. S2 in the Supplementary Material.

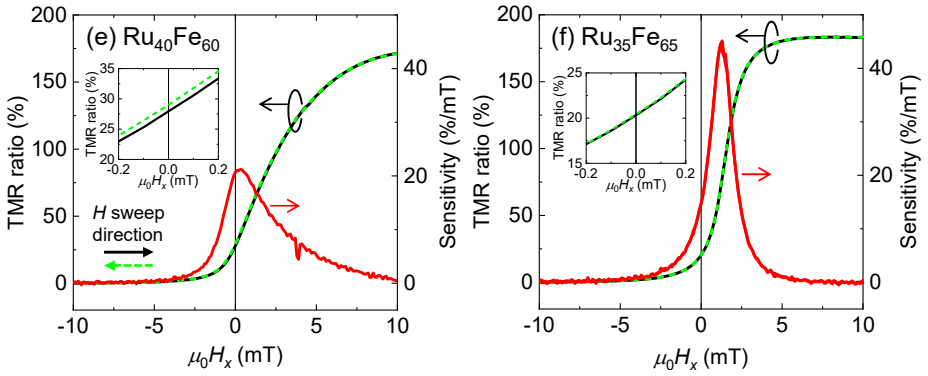

Revised Figs. 3(e) and (f)

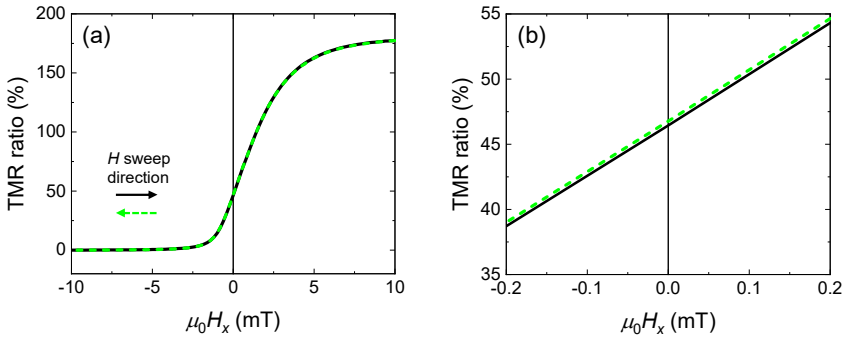

Fig. S2 in the supplementary material

3. Indicate RA and resistance of the devices

(Response) We have added the *RA* and *R* values of the devices in the experimental part.

(p.6, line 22-)

"The resistance-area product values in the parallel magnetization configuration (RA_p) of the devices were 20–200 kΩ μm^2 (A = 1,256 μm^2). Despite the variation in the RA_p value, which was due to batch-to-batch variation and non-uniformity within the substrate of the MgO thickness and quality, the TMR ratio was approximately constant at 180%."

4. I suggest removing the part on the GMR devices. Keep in mind this is a letter.

(Response) The GMR part (Fig. 1) shows important method and data to reproduce the results of this study. This provides a simple and reliable method to directly measure the noncollinear IEC angle (θ_{IEC}). Knowing θ_{IEC} is critical to obtain the appropriate value of θ_{ua} to obtain large sensitivity from the simulation, as shown in Fig. 3(d). (θ_{IEC} and θ_{ud} are equivalent in definition) Therefore, we must keep it. The word count of the manuscript (before revision) was less than 3000, the word limit for initial submission to APL.